JCTC Journal of Chemical Theory and Computation

ARTICLE

pubs.acs.org/JCTC

First Principles Simulations of the Infrared Spectrum of Liquid Water Using Hybrid Density Functionals

Cui Zhang,[†] Davide Donadio,[†,⊥] François Gygi,[‡,§] and Giulia Galli*[,†,∥]

[†]Department of Chemistry, University of California, Davis, California 95616, United States

[‡]Department of Applied Science, University of California, Davis, California 95616, United States

[§]Department of Computer Science, University of California, Davis, California 95616, United States

[∥]Department of Physics, University of California, Davis, California 95616, United States

Supporting Information

ABSTRACT: We show that first principles hybrid functional (PBE0) simulations of the infrared spectrum of liquid water yields a much better agreement with experimental results than a semilocal functional description; in particular, the quantitative accord with measured stretching and bending bands is very good. Such an improved description stems from two effects: a more accurate account, at the PBE0 level of theory, of the vibrational properties of the monomer and dimer and an underlying structural model for the liquid with a smaller number of hydrogen bonds and oxygen coordination than those obtained with semilocal functionals. The average electronic gap of the liquid is increased by 60% with respect to the PBE value, when computed at the PBE0 level of theory, and is in fair agreement with experimental results.

1. INTRODUCTION

Providing a theoretical description of the properties of liquid water and acquiring the ability to simulate them have been central topics in physical chemistry and the subject of intense activities for many decades. However, a description of hydrogen bonding in liquid water is still the subject of debate,[1−3] with controversies recently stirred, for example, by spectroscopic measurements[1] pointing at an oxygen coordination and the number of hydrogen bonds substantially smaller than those in ice.

Building on the pioneering work of Rahman and Stillinger,[4] molecular dynamics (MD) and Monte Carlo (MC) techniques have been extensively used to simulate water in different thermodynamic states, by using classical interatomic potentials fitted to specific sets of experimental data. A number of force fields has been employed, including simple point charge (SPC) models[5] (either rigid[6] or flexible[7−9]) or more sophisticated parametrizations such as TIP4P[10] and TIP5P.[11] Although useful and successful in describing a number of structural and dynamical properties of aqueous systems, classical potentials often lack transferability to thermodynamic conditions and environments different from those for which they were fitted; in addition, they cannot describe processes where bond breaking and formation occur, and they may not be used to analyze spectroscopic measurements where electronic effects play an important role, for example, vibrational spectra.[12] Developing theoretical frameworks capable of accounting not only for structural and thermodynamic properties but also for spectroscopic data is of the greatest importance to interpreting complex measurements and thus gaining insight into hydrogen bonding in the liquid.

The ability to account for electronic effects and carry out MD simulations where the electronic structure of liquid water, treated as a condensed system, is computed at each step of the dynamics came with the advent of the Car−Parrinello (CP) method.[13] This framework also opened the way to addressing spectroscopic properties from first principles. Within this approach, the electronic structure of the liquid is described with density functional theory (DFT), and different levels of approximations for the exchange correlation functional have been used. Among semilocal functionals, the most widely adopted are the gradient corrected functionals BLYP[14,15] and PBE.[16,17] The first simulation using BLYP appeared in 1993,[18] and it gave important, qualitative information about a DFT-based description of the structure of liquid water under ambient conditions. It has now been established by several authors[19−24] that if the electronic structure of the liquid is properly converged (that is, numerical inaccuracies present in some early simulations are eliminated), both PBE and BLYP functionals yield overstructured pair correlation functions $g_{OO}(r)$ under ambient conditions, as compared to experimental results, a self-diffusion constant that is greatly underestimated, and a number of hydrogen bonds that is most likely overestimated. The errors of PBE and BLYP on both structural and self-diffusion properties can be artificially "corrected" by a temperature shift of ∼50 to 100 K, depending on whether rigid or flexible water models[25,26] are employed.[27] Therefore, a DFT description with BLYP and PBE gradient corrected functionals can give a reasonably good, qualitative account of water structure, although the accord with experimental results is not fully quantitative. In addition, both PBE and BLYP functionals yield a reasonably good description of the vibrational properties of the liquid,[28−33] although a quantitative discrepancy with experimental results remains, for example, a sizable red shift of about 200 cm^{-1} of the infrared (IR) stretching

Received: February 9, 2011
Published: March 21, 2011

band, indicating that improvements in the description of hydrogen bonds in the liquid are necessary.

Such improvements may come from the use of a higher level of theory than provided by local and semilocal density functionals. Hybrid functionals have been used by several authors[34−38] to investigate the structural properties of the liquid. Substantial differences have been found between the PBE and BLYP descriptions and that provided by empirical functionals such as HCTH.[34] Two studies using approximate forms of the hybrid functionals PBE0[39] and B3LYP[40] have also appeared in the literature.[35,36] Todorova et al.[35] found a more diffusive and less structured liquid, at the PBE0 level of theory, than with PBE, in qualitative agreement with the report of Li et al.;[37] Guidon et al.[36] reported instead negligible differences between pair correlation functions computed with PBE and PBE0, indicating negligible changes in the number and character of hydrogen bonds found in the system. The study of water clusters reported in refs 41 and 42 is consistent with the findings of a less structured liquid within PBE0; indeed it was shown that PBE0 yields smaller binding energies[41,42] and smaller polarizabilities[43] than PBE. However, in ref 35, larger binding energies are reported when using PBE0. We note that approximations in the implementation of the exact exchange operator have been adopted in both refs 35 and ref 36 and that the two studies were carried out in different ensembles.[44]

The great majority of first principles simulations have so far neglected the quantum nature of the proton. The significance of treating the proton as a quantum mechanical particle has been recently investigated by Morrone and Car[45] using path integral (PI) simulations and a DFT description of the electronic structure with the BLYP functional. These authors showed that the agreement with experimental results for the liquid structural properties is improved when proton quantum effects are included, consistent with the results obtained with PI calculations and empirical potentials.[46] PI simulations have also been carried out using *ab initio* based potentials, finding an effect similar to that reported in ref 45, that is a softening of the oxygen−oxygen pair correlation function corresponding to less structured hydrogen bonded networks, when treating protons quantum mechanically.[47,48]

Most of the theoretical investigations at the DFT level (and all of those using nonlocal functionals) have focused on the structural properties of the liquid, with few studies of vibrational[22,29,31−33] and electronic[2,3,49−52] properties appearing in the past several years. In order to gain a better understanding of water and in particular of hydrogen bonding, it is important to develop tools to compute accurate spectroscopic quantities and thus compare directly with a wealth of available measurements, in addition to structure factors and pair correlation functions. The IR spectra of water were first studied at the PBE level by Sharma et al.,[29] yielding a qualitative agreement with experimental results. Subsequent studies[32,33] outlined the importance of intermolecular dipolar correlations in shaping the IR spectrum of the liquid, and in particular of the complex stretching band. However quantitative discrepancies between theory and experiments remain, for example, on the position of the IR stretching band, and the origin of these discrepancies is not well understood. For example, it is yet unknown how the inaccuracies in the description of the liquid structural properties and thus of hydrogen bonding found in first principles simulations impact our understanding of vibrational measurements.

In this paper, we focus on the vibrational spectroscopy of the liquid,[53] and we report IR spectra computed using the nonlocal functional PBE0. So far, no vibrational study of liquid water or ice using nonlocal functionals has appeared in the literature. We find a much better agreement with experimental results, especially in the description of the stretching and bending bands, than obtained with semilocal functionals (at the GGA level); two main reasons are responsible for our improved description: a better account of the vibrational properties of the monomer and dimer and an underlying structural model for the liquid with a smaller number of hydrogen bonds and a smaller effective molecular dipole than those obtained at the GGA level. These results have important implications for the study of vibrational properties of water in contact with surfaces. The rest of the paper is organized as follows: our methodological approach is presented in section 2, and our results are discussed in section 3, for both structural and vibrational properties. Section 4 contains our conclusions.

2. METHODS

We performed first principles molecular dynamics simulations of heavy water D_2O using the *Qbox* code,[54] with cubic cells containing 32 molecules, and all of our results for vibrational spectra have been obtained at a fixed density of 1.108 g/cm^3. We employed both semilocal (PBE) and hybrid (PBE0) exchange and correlation functionals. In the case of simulations using PBE, we compared our results with those obtained with a 96 molecule cell. The equilibrium density of water using PBE has been predicted to be 0.85−0.90 g/cm^3,[55,56] that is, ≃10−15% smaller than in experiments. We carried out simulations at this lower density with the PBE functional at ∼400 K, and we found a worse agreement with neutron diffraction data than at the experimental density. In particular, the liquid turned out to be more structured than at higher density, as indicated, e.g., by an analysis of the pair correlation function $g_{OO}(r)$ (see Figure 1 in the Supporting Information). Given these results and given that the equilibrium density of water at the PBE0 level of theory has not yet been determined, we carried out simulations of vibrational spectra at the experimental equilibrium density of deuterated water, and we defer investigations as a function of density to a later study. Although it is in principle possible to compute the equilibrium density of the liquid using the PBE0 functional, this would be computationally very intensive, as PBE0 calculations are substantially heavier, from a computational standpoint, than those using PBE.[57]

In all liquid simulations, we adopted a plane wave (PW) basis set and norm-conserving pseudopotentials (PP)[58] with a kinetic energy cutoff of 85 Ry. The computation of the Hartree−Fock exchange operator included in the PBE0 functional was carried out without truncation of the range of the Coulomb interaction, unlike in previous studies,[35,36] and in such a way to ensure quadratic convergence with respect to Brillouin zone integration. In particular, calculations performed at the Γ point of the Brillouin zone correctly include divergent terms stemming from the long range of the Coulomb potential. An efficient parallelization scheme implemented in *Qbox* mitigates the high computational cost of the Hartree−Fock exchange energy when using PW basis sets.[59] Simulations were carried out with a time step of 10 a.u. in the NVE ensemble at several temperatures (T) ranging from 370 to 470 K, within a Born−Oppenheimer (BO) framework. At each T, the system was equilibrated for at least 10 ps and

up to 20 ps, and trajectories were collected for 17 ps. The electronic contributions to the molecular dipole moment were computed using maximally localized Wannier functions[60] (MLWFs), evaluated at each MD step with the algorithm proposed in ref 61. The IR absorption coefficient per unit length was obtained within linear response theory from the Fourier transform of the time correlation function of the system's dipole moment:[62]

$$\alpha(\omega) = \frac{2\pi\omega^2\beta}{3cVn(\omega)}\int_{-\infty}^{\infty} dt e^{-i\omega t}\langle \sum_{ij} \vec{\mu_i}(0)\cdot\vec{\mu_j}(t)\rangle \qquad (1)$$

where $n(\omega)$ is the refractive index, V is the volume, $\beta = 1/k_B T$ is the inverse temperature, and $\vec{\mu}_i$ is the molecular dipole moment. Before discussing the IR spectra of liquid water, we present results obtained for the vibrational properties of the water monomer and dimer using the PBE and PBE0 functionals, and we discuss the effect of the basis set (energy cutoff) and PP on our results.

3. RESULTS AND DISCUSSION

3.1. Vibrational Properties of the Water Molecule and the Water Dimer. We first analyzed the effect of the PP used in our calculations by comparing results at the PBE and PBE0 levels of theory with all electron (AE) and experimental results for the H_2O molecule and the H_2O dimer (see details of the calculations in the Supporting Information). AE results are not available for the deuterated water molecule and dimer. We found that for converged basis sets (200 Ry) at the PBE level, PP and AE results differ by a few wavenumbers, showing the excellent performance of converged PP calculations. Deviation from AE results appears to be bigger in the case of PBE0 (up to 34 cm^{-1}), most likely because we have used PP generated within PBE.

Table 1. Vibrational Frequencies (cm^{-1}) of the Deuterated Water Monomer D_2O[a,b]

	Ecut (Ry)	pseudopotentials	ν_1	ν_2	ν_3
PBE	85	Hamann	2605	1164	2735
PBE	200	Hamann	2616	1165	2746
PBE	85	HSCV	2655	1164	2779
PBE	200	HSCV	2656	1165	2780
PBE0	85	Hamann	2717	1195	2850
PBE0	200	Hamann	2719	1199	2851
PBE0	85	HSCV	2763	1197	2890
PBE0	200	HSCV	2758	1199	2885
expt. harm.[65]			2764	1206	2889
expt. anharm.[65]			2671	1178	2788

[a] Simulations of the water molecule were carried out in a cubic cell with L = 30 Bohr. [b] ν_1, symmetric stretching; ν_2, bending; ν_3, asymmetric stretching.

In Tables 1 and 2, we show calculated vibrational frequencies of the D_2O molecule and the dimer obtained with two different norm-conserving PPs: Hamann[58] and Hamann–Schlüter–Chiang–Vanderbilt (HSCV).[63,64] As for H_2O, we compare our results to experimental harmonic frequencies, because calculations of vibrational frequencies at T = 0 by, e.g., finite differences, do not include anharmonic effects, unlike our MD simulation results at finite T, which account for classical anharmonic effects. For converged basis sets (200 Ry), all of the modes of the monomer are underestimated, with respect to experimental results, by up to 5.4% with the PBE functional, while converged PBE0 results are in excellent agreement with harmonic frequencies extracted from measured spectra.[65] Experimental harmonic frequencies are not available for low frequency modes of the dimers; however, from a comparison with anharmonic frequencies, and given the shape of the potential energy curve of the dimer, it is likely that both PBE and PBE0 slightly overestimate the low frequency modes (see Tables 3 and 4 in the Supporting Information).

In the case of intramolecular frequencies of $(D_2O)_2$ within PBE0, the comparison with harmonic frequencies extracted from experimental data[66] shows that stretching frequencies are slightly underestimated when using Hamann PP with a converged basis set (200 Ry), with the errors on the donor being slightly larger than those on the acceptor. HSCV PP yields instead a slight overestimate of the stretching frequencies. Bending frequencies are consistently underestimated by 9–10 cm^{-1} with either type of PP.

The computed binding energy of the dimer is 5.12 kcal/mol with PBE0 and 5.24 kcal/mol with PBE, in good agreement with the data obtained with AE calculations and Gaussian basis sets.[68] We find that the difference between the binding energies obtained with the two functionals, $\Delta E_{binding} = E^{PBE}_{binding} - E^{PBE0}_{binding}$, is 0.12 kcal/mol, to be compared with 0.15 kcal/mol from ref 68. Overall, our results for the vibrational frequencies of the water monomer and dimer show that the PBE0 functional very much improves the description obtained at the PBE level, and thus it appears to be a promising exchange correlation functional to

Table 2. Vibrational Frequencies (cm^{-1}) of the Deuterated Water Dimer $(D_2O)_2$[a,b]

	Ecut (Ry)	pseudopotentials	ν_1	ν_2	ν_3	ν_4	ν_5	ν_6
PBE	85	Hamann	2601	1164	2698	2492	1176	2729
PBE	200	Hamann	2613	1165	2710	2510	1177	2741
PBE	85	HSCV	2650	1164	2772	2549	1175	2744
PBE	200	HSCV	2652	1165	2774	2549	1176	2745
PBE0	85	Hamann	2714	1196	2845	2624	1208	2817
PBE0	200	Hamann	2716	1199	2846	2631	1212	2819
PBE0	85	HSCV	2759	1196	2885	2673	1207	2859
PBE0	200	HSCV	2754	1199	2879	2666	1211	2853
expt. harm.[66]			2738	1209	2857	2689	1221	2838
expt. anharm.[67]			2650	1182	2757	2599	1193	2738

[a] Simulations of the water dimer were carried out in a cubic cell with L = 30 Bohr. [b] ν_1, symmetric stretching of acceptor; ν_2, bending of acceptor; ν_3, asymmetric stretching of acceptor; ν_4, symmetric stretching of donor; ν_5, bending of donor; ν_6, asymmetric stretching of donor.

dx.doi.org/10.1021/ct2000952 |J. Chem. Theory Comput. 2011, 7, 1443–1449

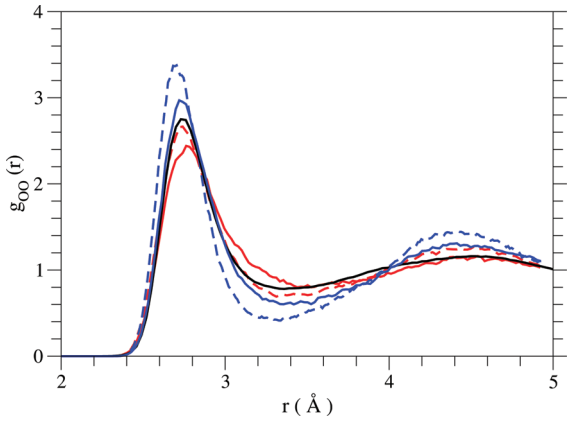

Figure 1. Comparison of oxygen−oxygen pair correlation functions for systems consisting of 32 water molecules, obtained with the PBE0 functional at 438 ± 29 K (solid red) and 374 ± 27 K (solid blue), and the PBE functional at 439 ± 29 K (dash red) and 367 ± 25 K (dash blue). The experimental result at room temperature is displayed by the black line.[70]

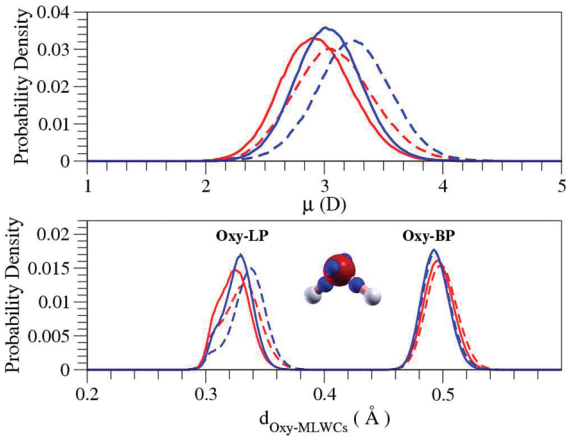

Figure 2. Distributions of molecular dipole moments and distances between oxygen and maximally localized Wannier centers (MLWCs), obtained with the PBE0 functional at 438 ± 29 K (solid red) and 374 ± 27 K (solid blue), and the PBE functional at 439 ± 29 K (dash red) and 367 ± 25 K (dash blue). The inset shows the positions of the centers of maximally localized Wannier functions in a water molecule. The two orbitals centered close to the OD bonds are bond pair (BP) orbitals; the other two are lone pair (LP) orbitals.

study the vibrational properties of liquid water. Our results for the liquid are presented in the next section using an 85 Ry cutoff and the Hamann PP,[69] after comparing structural properties obtained with PBE and PBE0 functionals.

3.2. Vibrational Properties and Hydrogen Bonding of Liquid Deuterated Water. Figure 1 shows the oxygen−oxygen pair correlation functions $g_{OO}(r)$ at two different temperatures slightly below and above 400 K, obtained with the PBE and PBE0 functionals. (We recall that within PBE, at the experimental density, we obtain a good agreement with the measured pair correlation function at room temperature by shifting the simulation temperature to about 400 K). The result of PBE calculations carried out with the cell containing 96 molecules yields a pair correlation function $g_{OO}(r)$ which, within error bars,[20] is the same as that obtained with 32 molecules (see Figure 2 in the Supporting Information). Pair correlation functions computed using the Hamann and HSCV PPs and 32 molecule cells are also the same, within error bars (see Figure 3 in the Supporting Information). A comparison between PBE and PBE0 results at the two temperatures reported in Figure 1 clearly shows that the PBE0 functional improves over the PBE description, yielding a much less structured pair correlation function. Our findings are consistent (though not in close agreement) with those of ref 35, showing differences between PBE and PBE0 results for $g_{OO}(r)$, but they are at variance with the results of ref 36, which found hardly any change when carrying out calculations of structural properties at the PBE and PBE0 levels of theory.[71] The structural differences found here are consistent with a decrease of the molecular dipole moment found when using PBE0 (see Figure 2, upper panel). The calculated average molecular dipole moments with PBE0 are 2.88 ± 0.30 D (at 471 K), 2.94 ± 0.30 D (at 438 K), and 3.06 ± 0.29 D (at 374 K), and the corresponding ones with PBE are 3.03 ± 0.35 D (at 470 K), 3.09 ± 0.34 D (at 439 K), and 3.24 ± 0.32 D (at 367 K). An effective dipole moment of 2.9 ± 0.6 D has been derived from X-ray measurements,[72] which is consistent with both our calculations and the value of the dipole extracted for water clusters with six molecules (2.7 D).[73] Our findings for the liquid are also consistent with our results on the binding energy of the dimer, which is smaller with PBE0 than PBE.

The calculated structural differences between PBE0 and PBE stem from a decrease in the average number of hydrogen bonds when using the hybrid functional: 3.26 vs 3.43 at ∼438 K and 3.60 vs 3.79 at ∼374 K. Hydrogen bonds are defined using a geometrical criterion: two molecules are regarded as hydrogen bonded if the OO distance is less than 3.35 Å, and the O−OD angle is less than 30° (see Table 5 in the Supporting Information for further details). Differences in hydrogen bonding are also shown by the distribution of distances between oxygen and the centers of the MLWFs, displayed in Figure 2, lower panel. Two MLWFs are centered along OD bonds, and we call them bond pair (BP) orbitals. The other two are approximately centered on symmetric tetrahedral sites, and we call these lone pair (LP) orbitals. The four centers of the MLWFs of a water molecule are shown in the inset of Figure 2, lower panel. It is seen that the distributions of Oxy−BP distances are very similar when using PBE and PBE0, while those of Oxy−LP distances show marked differences.

In particular, the average distance between oxygen atoms and Wannier centers of the LP orbitals is shorter when computed with PBE0 than with PBE; in addition, the shoulder on the left-hand side of the Oxy−LP distance distribution, associated with single acceptor hydrogen bonds, is more pronounced. This indicates that at the PBE0 level, liquid water exhibits a more distorted hydrogen bonded network, with a larger number of broken hydrogen bonds. We also note that in addition to improving structural properties, calculations with the PBE0 functional yield differences in the electronic structure of the fluid, with an average electronic band gap of 6.73 eV, to be compared with the PBE value of 4.23 eV. However, also within PBE0, we obtain a value which is underestimated compared with experimental results (8.7 eV).[74]

We now turn to discussing our results for the vibrational spectrum of the liquid, as a function of temperature. The IR spectra of liquid deuterated water computed with the PBE and PBE0 functionals are compared with experimental results in Figure 3. The improvement of the PBE0 description with respect

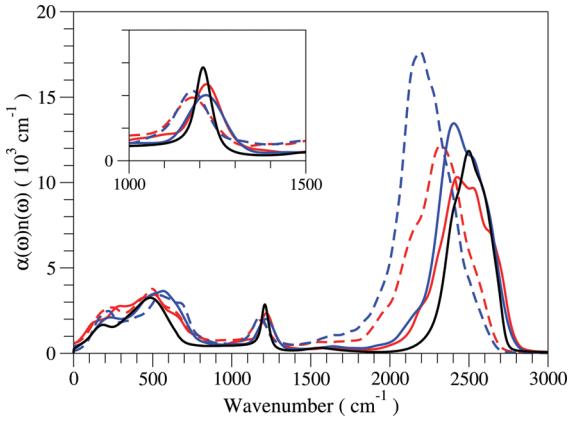

Figure 3. Calculated IR spectra of liquid D_2O with the PBE0 functional at 438 ± 29 K (solid red) and 374 ± 27 K (solid blue), compared with the ones calculated with the PBE functional at 439 ± 29 K (dash red) and 367 ± 25 K (dash blue). The experimental spectrum at room temperature is displayed by the black line.[75] The inset shows the spectra in the range 1000 cm^{-1} to 1500 cm^{-1}.

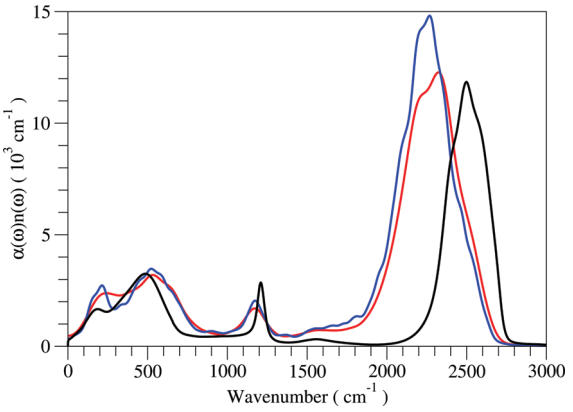

Figure 4. Calculated IR spectra of liquid D_2O with the PBE functional for systems consisting of 32 water molecules at 408 ± 27 K (red) and 96 water molecules at 407 ± 16K (blue), compared with the experimental spectrum at room temperature[75] (black).

to PBE over the entire spectrum is apparent, especially so for the positions of the stretching and bending bands (see inset in Figure 3). This improvement comes from the combined effect of a better description of the frequencies of the monomer and dimer (see section 3.1) and an improved description of the structure of the liquid, with a smaller average molecular dipole moment corresponding to reduced strength of the hydrogen bonds. Weaker hydrogen bonding leads to stiffer intramolecular covalent bonds and higher stretching and bending frequencies. The positions of band maxima corresponding to hindered translations, librations, bending, and stretching modes computed with the PBE0 functional at 438 K are 180 (186, 246), 503 (486, 497), 1219 (1209, 1179), and 2426 (2498, 2322) cm^{-1}, respectively, where wavenumbers in parentheses are experimental values at room temperature[75] and results calculated with the PBE functional at 439 K, respectively. The corresponding values with PBE0 at 374 K are are 211 (186, 219), 579 (486, 549), 1211 (1209, 1179), and 2388 (2498, 2192) cm^{-1}, respectively, where wavenumbers in parentheses have the same meaning as those at 438 K. With the PBE0 functional, the red shift of the calculated stretching band with respect to experimental results is reduced to 72 cm^{-1} at ∼438 K and 110 cm^{-1} at ∼374 K, compared with 176 cm^{-1} and 306 cm^{-1} obtained with the PBE functional, respectively. We expect that the use of a PBE0 PP would bring our PBE0 results in closer agreement with experimental results, based on the comparison shown in Tables 1 and 2 in the Supporting Information. The comparison of our results to experimental ones for the low frequency band is more delicate as our sample is rather small. We note that a comparison of calculations at the PBE level of theory carried out with 32 and 96 molecules (see Figure 4) shows modest size effects for the stretching and bending bands.

The intensity of the stretching band calculated with the PBE0 functional is significantly smaller compared to the one computed at the PBE level. The ratio between the experimental intensities of ice[76] and water[75] stretching bands, after rescaling T, is approximately 1.3, suggesting that the less hydrogen bonded the system, the less intense the IR stretching band. This is consistent with the PBE0 intensity being smaller than the PBE one, at the same T. In addition to a blue-shifted main peak, the stretching band obtained with PBE0 shows a more pronounced shoulder at higher frequencies, compared with the spectrum obtained with PBE at the same temperature. This is again due to the increased number of broken hydrogen bonds in the liquid. As discussed in ref 33, within PBE, the contribution to the IR stretching band from molecules with broken hydrogen bonds gives rise to a shoulder at higher frequencies but not to a distinctive peak. This shoulder is more pronounced when using the hybrid functional, as expected from a less structured and less hydrogen bonded fluid. However, we emphasize that in the liquid, irrespective of which description is used (semilocal or hybrid functionals), hydrogen bonds are broken only for a short time, thus a clear IR signal associated to steadily broken bonds is not present in vibrational spectra. Also, the line shape of the bending modes is significantly improved within PBE0, consistent with the improved description of bending modes in the water molecule and dimer. Finally, we note that the analysis of the relative contributions of inter- and intramolecular correlations to the IR stretching band reported in ref 33 holds at the PBE0 level as well.

The results reported in Figure 3 show that the positions of the bending and stretching peaks are both blue-shifted when T is increased. An increase of temperature may mimic, to some extent, the effect one would find by including a quantum mechanical description of the deuterons. More delocalized deuterons may weaken hydrogen bonds and thus enhance the signature of molecules with broken or distorted hydrogen bonds, which yield a blue-shifted IR signal, compared to that of perfectly hydrogen bonded molecules. The centroid MD simulations reported in refs 47 and 77 found instead a red shift in the position of the stretching band, with respect to classical MD. However, these results appear to be controversial;[78,79] indeed, it was recently pointed out that the observed red shift may be an artifact of the centroid MD technique.

4. CONCLUSIONS

We have shown that when using the PBE0 functional to describe the electronic structure of liquid water within DFT, one obtains structural and vibrational properties in better agreement with experimental results than calculations done with PBE and, in general, with semilocal functionals. In particular, we find a less structured fluid, with a lower dipole moment associated with

each molecule and a higher number of fleetingly broken or distorted hydrogen bonds. We also find the IR spectrum to be in closer agreement with recent measurements,[75] showing a more pronounced shoulder corresponding to temporarily broken hydrogen bonds. The improved agreement with experimental results found for the spectrum stems from an improved description of both the structure of the liquid and the monomer and dimer vibrational frequencies. We believe that our findings represent a significant step forward in the theoretical modeling of water from first principles, as one may now extend the framework adopted here to other aqueous environments, such as water in contact with surfaces and simple aqueous solutions, thus opening the way to complement and interpret many spectroscopic measurements in an accurate fashion. In addition, encouraging results were found for electronic properties as well, and work is in progress to investigate in detail the electronic structure of the liquid using hybrid functionals.

However, several issues in the description of both structural and vibrational properties of water remain to be addressed, including the determination of the equilibrium density of water and its melting temperature when using hybrid functionals. In addition, it would be interesting to quantitatively assess the significance of proton quantum effects on vibrational spectra, when using a DFT-PBE0 description of the fluid. On the basis of the findings of ref 45, we expect the inclusion of proton quantum effects on our PBE0 results would lead to a less structured fluid, bringing the pair correlation function in even better agreement with experimental results. Our results on changes of IR spectra as a function of T, showing a blue shift of bending and stretching peaks as T is increased, indicate that the inclusion of proton quantum effects may improve the description of vibrations as well, although a detailed analysis is clearly needed to draw any firm conclusion.

While the qualitative effect on structural properties of treating the proton quantum mechanically is relatively straightforward to predict, an understanding of the influence of a more accurate description of van der Waals and dispersion forces is still under debate. Investigations of water clusters have so far shown critical dependence of results (e.g., order of energetically favored configurations) on the so-called dispersion corrections used[42,80] on top of simulations within DFT-PBE. Although no firm conclusion has yet been reported for liquid water, it appears that adding dispersion contributions to semilocal density functionals leads to a less structured liquid;[55,56,81] however, several open problems remain, e.g., in the description of the second solvation shell (next-nearest neighbor structural properties).

■ ASSOCIATED CONTENT

Ⓢ Supporting Information. Vibrational frequencies, average number of hydrogen bonds, and calculated oxygen−oxygen pair correlation functions. This material is available free of charge via the Internet at http://pubs.acs.org/.

■ AUTHOR INFORMATION

Corresponding Author

*E-mail: gagalli@ucdavis.edu.

Present Addresses

⊥Max Planck Institute for Polymer Research, 55128 Mainz, Germany

■ ACKNOWLEDGMENT

We would like to thank Ivan Duchemin and Roberto Car for helpful discussions. This work was supported by NSF Grant OCI-0749217. Use of ALCF computational resources at Argonne National Laboratory is gratefully acknowledged.

■ REFERENCES

(1) Wernet, Ph.; Nordlund, D.; Bergmann, U.; Cavalleri, M.; Odelius, M.; Ogasawara, H.; Näslund, L. Å.; Hirsch, T. K.; Ojamäe, L.; Glatzel, P.; Pettersson, L. G. M.; Nilsson, A. *Science* **2004**, *304*, 995–999.
(2) Prendergast, D.; Galli, G. *Phys. Rev. Lett.* **2006**, *96*, 215502.
(3) Chen, W.; Wu, X.; Car, R. *Phys. Rev. Lett.* **2010**, *105*, 017802.
(4) Rahman, A.; Stillinger, F. H. *Phys. Rev. A* **1974**, *10*, 368–378.
(5) Berendsen, H. J. C.; Postma, J. P. M.; van Gunsteren, W. F.; Hermans, J. In *Intermolecular Forces*; Pullman, B., Ed.; Reidel: Dordrecht, The Netherlands, 1981; p 331.
(6) Berendsen, H. J. C.; Grigera, J. R.; Straatsma, T. P. *J. Phys. Chem.* **1987**, *91*, 6269–6271.
(7) Toukan, K.; Rahman, A. *Phys. Rev. B* **1985**, *31*, 2643–2648.
(8) Dang, L. X.; Pettitt, B. M. *J. Phys. Chem.* **1987**, *91*, 3349–3354.
(9) Wu, Y.; Tepper, H. L.; Voth, G. A. *J. Chem. Phys.* **2006**, *124*, 024503.
(10) Jorgensen, W. L.; Chandrasekhar, J.; Madura, J. D.; Impey, R. W.; Klein, M. L. *J. Chem. Phys.* **1983**, *79*, 926–935.
(11) Mahoney, M. W.; Jorgensen, W. L. *J. Chem. Phys.* **2000**, *112*, 8910–8922.
(12) Donadio, D.; Cicero, G.; Schwegler, E.; Sharma, M.; Galli, G. *J. Phys. Chem. B* **2009**, *113*, 4170–4175.
(13) Car, R.; Parrinello, M. *Phys. Rev. Lett.* **1985**, *55*, 2471–2474.
(14) Becke, A. D. *Phys. Rev. A* **1988**, *38*, 3098–3100.
(15) Lee, C.; Yang, W.; Parr, R. G. *Phys. Rev. B* **1988**, *37*, 785–789.
(16) Perdew, J. P.; Burke, K.; Ernzerhof, M. *Phys. Rev. Lett.* **1996**, *77*, 3865–3868.
(17) Perdew, J. P.; Burke, K.; Ernzerhof, M. *Phys. Rev. Lett.* **1997**, *78*, 1396.
(18) Laasonen, K.; Sprik, M.; Parrinello, M.; Car, R. *J. Chem. Phys.* **1993**, *99*, 9080–9089.
(19) Asthagiri, D.; Pratt, L. R.; Kress, J. D. *Phys. Rev. E* **2003**, *68*, 041505.
(20) Grossman, J. C.; Schwegler, E.; Draeger, E. W.; Gygi, F.; Galli, G. *J. Chem. Phys.* **2004**, *120*, 300–311.
(21) Schwegler, E.; Grossman, J. C.; Gygi, F.; Galli, G. *J. Chem. Phys.* **2004**, *121*, 5400–5409.
(22) Sit, P. H.-L.; Marzari, N. *J. Chem. Phys.* **2005**, *122*, 204510.
(23) Fernández-Serra, M. V.; Artacho, E. *J. Chem. Phys.* **2004**, *121*, 11136–11144.
(24) Kühne, T. D.; Krack, M.; Parrinello, M. *J. Chem. Theory Comput.* **2009**, *5*, 235–241.
(25) Allesch, M.; Schwegler, E.; Gygi, F.; Galli, G. *J. Chem. Phys.* **2004**, *120*, 5192–5198.
(26) Leung, K.; Rempe, S. B. *Phys. Chem. Chem. Phys.* **2006**, *8*, 2153–2162.
(27) In a so-called rigid water model, the O−H bond length and the H−O−H bond angle are constrained to be fixed during the simulation; in a flexible water model, all ionic degrees of freedom are allowed to vary.
(28) Silvestrelli, P. L.; Bernasconi, M.; Parrinello, M. *Chem. Phys. Lett.* **1997**, *277*, 478–482.
(29) Sharma, M.; Resta, R.; Car, R. *Phys. Rev. Lett.* **2005**, *95*, 187401.
(30) Iftimie, R.; Tuckerman, M. E. *J. Chem. Phys.* **2005**, *122*, 214508.
(31) Lee, H.-S.; Tuckerman, M. E. *J. Chem. Phys.* **2007**, *126*, 164501.
(32) Chen, W.; Sharma, M.; Resta, R.; Galli, G.; Car, R. *Phys. Rev. B* **2008**, *77*, 245114.
(33) Zhang, C.; Donadio, D.; Galli, G. *J. Phys. Chem. Lett.* **2010**, *1*, 1398–1402.
(34) VandeVondele, J.; Mohamed, F.; Krack, M.; Hutter, J.; Sprik, M.; Parrinello, M. *J. Chem. Phys.* **2005**, *122*, 014515.

(35) Todorova, T.; Seitsonen, A. P.; Hutter, J.; Kuo, I.-F. W.; Mundy, C. J. *J. Phys. Chem. B* **2006**, *110*, 3685–3691.
(36) Guidon, M.; Schiffmann, F.; Hutter, J.; VandeVondele, J. *J. Chem. Phys.* **2008**, *128*, 214104.
(37) Li, Z.; Wu, X.; Car, R. http://meetings.aps.org/Meeting/MAR10/Event/119032 (accessed March 2011).
(38) Guidon, M.; Hutter, J.; VandeVondele, J. *J. Chem. Theory Comput.* **2010**, *6*, 2348–2364.
(39) Adamo, C.; Barone, V. *J. Chem. Phys.* **1999**, *110*, 6158–6170.
(40) Becke, A. D. *J. Chem. Phys.* **1993**, *98*, 5648–5652.
(41) Santra, B.; Michaelides, A.; Scheffler, M. *J. Chem. Phys.* **2007**, *127*, 184104.
(42) Santra, B.; Michaelides, A.; Fuchs, M.; Tkatchenko, A.; Filippi, C.; Sheffler, M. *J. Chem. Phys.* **2008**, *129*, 194111.
(43) Xu, X.; Goddard, W. A. *J. Phys. Chem. A* **2004**, *108*, 2305–2313.
(44) Reference 35 reports simulations within the NVT ensemble, and ref 36 reports simulations within the NVE ensemble. In ref 36, a multiple time step scheme was used.
(45) Morrone, J. A.; Car, R. *Phys. Rev. Lett.* **2008**, *101*, 017801. The results presented in this paper differ from earlier PI simulations within DFT reported by Chen et al.[82] However, they are consistent with a large body of PI simulations carried out with classical or ab initio derived potentials. It is possible that the results of Chen et al. may suffer from inaccuracies in the comparison between classical and quantum simulations deriving from the choice of technical parameters in their simulations.
(46) Kuharski, R. A.; Rossky, P. J. *J. Chem. Phys.* **1985**, *82*, 5164–5177.
(47) Paesani, F.; Iuchi, S.; Voth, G. A. *J. Chem. Phys.* **2007**, *127*, 074506.
(48) Fanourgakis, G. S.; Xantheas, S. S. *J. Chem. Phys.* **2008**, *128*, 074506.
(49) Hetényi, B.; Angelis, F. D.; Giannozzi, P.; Car, R. *J. Chem. Phys.* **2004**, *120*, 8632–8637.
(50) Prendergast, D.; Grossman, J. C.; Galli, G. *J. Chem. Phys.* **2005**, *123*, 014501.
(51) Fernández-Serra, M. V.; Artacho, E. *Phys. Rev. Lett.* **2006**, *96*, 016404.
(52) Kulik, H. J.; Marzari, N.; Correa, A. A.; Prendergast, D.; Schwegler, E.; Galli, G. *J. Phys. Chem. B* **2010**, *114*, 9594–9601.
(53) Bakker, H. J.; Skinner, J. L. *Chem. Rev.* **2010**, *110*, 1498–1517.
(54) Qbox code. http://eslab.ucdavis.edu/software/qbox (accessed March 2011).
(55) Schmidt, J.; VandeVondele, J.; Kuo, I.-F. W.; Sebastiani, D.; Siepmann, J. I.; Hutter, J.; Mundy, C. J. *J. Phys. Chem. B* **2009**, *113*, 11959–11964.
(56) Wang, J.; Román-Pérez, G.; Soler, J. M.; Artacho, E.; Fernández-Serra, M.-V. *J. Chem. Phys.* **2011**, *134*, 024516.
(57) For 32 molecule cells, the ratio of the CPU time per MD step using PBE0 and PBE is about a factor of 25.
(58) Hamann, D. R. *Phys. Rev. B* **1989**, *40*, 2980–2987.
(59) Duchemin, I.; Gygi, F. *Comput. Phys. Commun.* **2010**, *181*, 855–860.
(60) Marzari, N.; Vanderbilt, D. *Phys. Rev. B* **1997**, *56*, 12847–12865.
(61) Gygi, F.; Fattebert, J. L.; Schwegler, E. *Comput. Phys. Commun.* **2003**, *155*, 1–6.
(62) Ramírez, R.; López-Ciudad, T.; Kumar-P, P.; Marx, D. *J. Chem. Phys.* **2004**, *121*, 3973–3983.
(63) Pseudopotential Table. http://fpmd.ucdavis.edu/potentials (accessed March 2011).
(64) Vanderbilt, D. *Phys. Rev. B* **1985**, *32*, 8412–8415.
(65) Benedict, W. S.; Gailar, N.; Plyler, E. K. *J. Chem. Phys.* **1956**, *24*, 1139–1165.
(66) Fredin, L.; Nelander, B.; Ribbegard, G. *J. Chem. Phys.* **1977**, *66*, 4065–4072.
(67) Tursi, A. J.; Nixon, E. R. *J. Chem. Phys.* **1970**, *52*, 1521–1528.
(68) Santra, B.; Michaelides, A.; Scheffler, M. *J. Chem. Phys.* **2009**, *131*, 124509.
(69) Although the HSCV PP yields results in slightly better agreement with AE calculations than the Hamann PP, we used the latter here, in order to be able to compare them to our previous results[33] for IR spectra, obtained with the Hamann PP.
(70) Soper, A. K. *Chem. Phys.* **2000**, *258*, 121–137.
(71) In refs 35 and 36, a cutoff function of the type $erfc(\alpha r)/r$ was adopted for the screened Coulomb operator; different values of α were used in the two papers. The functionals used in refs 35 and 36 are therefore different from the PBE0 one as commonly defined. Another difference between our simulation and those of refs 35 and 36 is the length of the trajectories (10(5) ps and 7 ps in refs 35 and 36, respectively, and 17 ps in our studies) and the equilibration procedure. The simulations of ref 35 contain 32 water molecules and are performed within the NVT ensemble at 350 K, while those of ref 36 contain 64 water molecules and are carried out within the NVE ensemble at 325 K.
(72) Badyal, Y. S.; Saboungi, M.-L.; Price, D. L.; Shastri, S. D.; Haeffner, D. R.; Soper, A. K. *J. Chem. Phys.* **2000**, *112*, 9206–9208.
(73) Gregory, J. K.; Clary, D. C.; Liu, K.; Brown, M. G.; Saykally, R. J. *Science* **1997**, *275*, 814–817.
(74) Bernas, A.; Ferradini, C.; Jay-Gerin, J.-P. *Chem. Phys.* **1997**, *222*, 151–160.
(75) Max, J.-J.; Chapados, C. *J. Chem. Phys.* **2009**, *131*, 184505.
(76) Bergren, M. S.; Schuh, D.; Sceats, M. G.; Rice, S. A. *J. Chem. Phys.* **1978**, *69*, 3477–3482.
(77) Fanourgakis, G. S.; Xantheas, S. S. *J. Chem. Phys.* **2008**, *128*, 074506.
(78) Ivanov, S. D.; Witt, A.; Shiga, M.; Marx, D. *J. Chem. Phys.* **2010**, *132*, 031101.
(79) Paesani, F.; Voth, G. A. *J. Chem. Phys.* **2010**, *132*, 014105.
(80) Kelkkanen, A. K.; Lundqvist, B. I.; Nørskov, J. K. *J. Chem. Phys.* **2009**, *131*, 046102.
(81) Lin, I.-C.; Seitsonen, A. P.; Coutinho-Neto, M. D.; Tavernelli, I.; Rothlisberger, U. *J. Phys. Chem. B* **2009**, *113*, 1127–1131.
(82) Chen, B.; Ivanov, I.; Klein, M. L.; Parrinello, M. *Phys. Rev. Lett.* **2003**, *91*, 215503.

NOTE ADDED AFTER ASAP PUBLICATION

This paper was published on the Web on March 21, 2011, with minor errors in references 15 and 72. The corrected version was reposted on March 31, 2011.